Accepted Manuscript

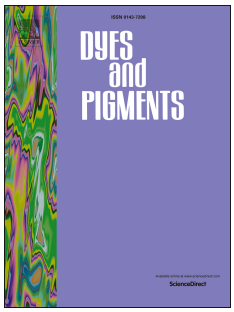

"Turn on" fluorescence response of monomethine cyanines caused by noncovalent binding to ct-DNA

Andrew Levitz, Cory Holder, Eduardo Soriano, Maged Henary

PII: S0143-7208(17)30435-7

DOI: 10.1016/j.dyepig.2017.05.051

Reference: DYPI 6013

To appear in: *Dyes and Pigments*

Received Date: 1 March 2017

Revised Date: 25 April 2017

Accepted Date: 29 May 2017

Please cite this article as: Levitz A, Holder C, Soriano E, Henary M, "Turn on" fluorescence response of monomethine cyanines caused by noncovalent binding to ct-DNA, *Dyes and Pigments* (2017), doi: 10.1016/j.dyepig.2017.05.051.

"Turn on" fluorescence response of monomethine cyanines caused by noncovalent binding to ct-DNA

Andrew Levitz[‡], Cory Holder[‡], Eduardo Soriano and Maged Henary[*]

Department of Chemistry, Georgia State University, Atlanta, GA 30302, USA

[‡] These authors contributed equally.

[*] To whom correspondence should be addressed.

*__Corresponding Author__:

Maged Henary, Ph.D.

100 Piedmont Ave. #315

Atlanta, GA 30303

Office: 404-413-5566; Fax: 404-413-5505

Email: mhenary1@gsu.edu

Abstract

Monomethine cyanines have been extensively studied for their use as probes for nucleic acids among other biological systems. Four monomethine cyanine dyes were synthesized with various heterocyclic moieties including quinoline, benzoxazole, benzothiazole, and 3,3-dimethylindolenine adjoining benz[*c*,*d*]indol-1-ium, which was found to directly influence their optical and energy profiles. The dyes were characterized by ^{1}H and ^{13}C NMR and HRMS. In this study the twisted conformation unique to monomethine cyanines was exploited in DNA binding studies where the benzoxazole containing sensor displayed up to 700-fold increase in fluorescence when bound to the DNA compared to the unbound form.

1. Introduction

In 1856 C.H.G. Williams heated quinolone with *N*-amyl lepidinium iodide in ammonia producing a “magnificent blue color” referred to in latin as *cyanos* thus the first cyanine dye was synthesized.[1] This vast class of dyes shows absorption that covers a wider range of the electronic spectrum than any other class of dyes, but due to their sensitivity to light the unimaginable value of cyanines was not discovered until 20 years later when they were employed to increase the sensitivity of the photographic plate. Since then cyanine dyes have been used in an incredible amount of applications including bioimaging,[2-4] solar cells,[5,6] and data storage[7] among other applications [8-12].

Cyanines are distinguished from other dyes in that they possess two nitrogen containing heterocycles that are connected by a conjugated methine bridge. The delocalization of electrons through this system gives them their characteristically high molar absorptivities and quantum yields. Their names depend on the number of methine groups found in the bridge connecting the two heterocycles. Monomethine dyes which include one methine group in the bridge tend to absorb in the 400-500 nm range of the visible region.

Imaging of macromolecules such as DNA by staining with fluorescent compounds is of great interest; therefore, expanding the options of available probes is vital to several areas of research spanning from medical diagnostics to genomics. The synthesis of low cost, easy to manipulate systems for fast analysis is required.[13] Fluorescent detection has rapidly become one of the most widely used techniques due to its sensitivity and noninvasiveness.[14] Ethidium bromide has commonly been used for the detection of DNA, however it has mutagenic effects and poses other environmental concerns.[15-17] On the other hand, cyanine dyes are sensitive, safe and highly modifiable.[18-20]

As described previously by our group, monomethine cyanines possess a valuable characteristic of only displaying fluorescence when rotation around the methine bridge is restricted.[18,21] These dyes are the best non-convalent binding nucleic acid labels due to their high binding constants, large molar absorptivities and quantum yields and high fluorescence signals upon binding. Two commercially available monomethine cyanines are among the most popular intercalating agents and have recently been used for DNA and chromatin imaging with super-resolution fluorescence microscopy.[22] While there is still much to explore regarding what effect structure has on the photophysical properties, our lab has developed ways to redshift the monomethine scaffold by altering the terminal heterocycles.[18,21] Understanding how to redshift the monomethine cyanine dyes allows for the enhancement of existing molecular probes minimizing background absorption and fluorescence. While it is well known that monomethine cyanines tend to bind DNA[23-25] there is a lack of literature on what causes or prevents a cyanine from binding to DNA. Calf thymus DNA (ct-DNA) is a heterogenous collection of linear fragments of mammalian DNA that is readily available and therefore commonly used for *in vitro* biological experimentation. Herein a series of monomethine cyanines that differ only in one heterocycle were synthesized to investigate how these different heterocycles influence DNA binding.

2. Results and Discussion

2.1 Synthesis

Toward correlating the various heterocyclic moieties and their ability to bind DNA, we began to rationally design monomethine cyanines containing the benz[*c,d*]indole heterocycle on one half of the dye. The other side possessed different heterocycles including 2-

methylbenzothiazole, 2-methylbenzoxazole, 2-methylquinoline, or 3,3-dimethylindole, heterocycles all with butyl side chains on the nitrogen. As shown in Table 1, the physicochemical properties of these four compounds are all very similar with molecular weight from 397-423 (without counterion) and polarizability from 76-80. They are all hydrophobic molecules with LogP between 7 and 10. With the exception of the benzoxazole containing dye they have similar topological polar surface area (TPSA). The oxygen atom typically raises the TPSA, but there is no way to keep it in line with the other compounds without altering the structure drastically. Due to the similarity of their physicochemical properties any change observed in binding to DNA should be based on the 3D structure of each dye.

Table 1. Physicochemical properties of monomethine cyanines

Dye	MW (amu)	LogP	TPSA ($Å^2$)	Polarizability
OX	397.54	7.68	5.479	76.21
BTZ	413.60	8.25	1.674	77.39
Q	407.58	8.69	1.165	78.36
IN	423.62	9.23	1.752	80.37

* Structures shown in Scheme 1 below

The asymmetrical red-shifted monomethine cyanine dyes were synthesized as shown in Scheme 1. The key intermediate **4** was synthesized beginning with the alkylation of benz[*c,d*]indol-2(1H)-one **1** by reflux with iodobutane in acetonitrile. The alkylated ketone **2** was then converted to the thioketone **3** under reflux with phosphorous pentasulfide in pyridine before methylation to a thioether with iodomethane creating the key precursor, quaternary ammonium salt **4**, which was used as one heterocycle for all the monomethine compounds. The other heterocycle included 2-methylbenzothiazole, 2-methylbenzoxazole, 2,3,3-trimethylindole, and 2-methylquinoline. These heterocycles were alkylated, respectively, with iodobutane in acetonitrile to form quaternary ammonium salts **5**. The two heterocycles **4** and **5** were condensed in acetonitrile with triethylamine to afford final dyes **6**.

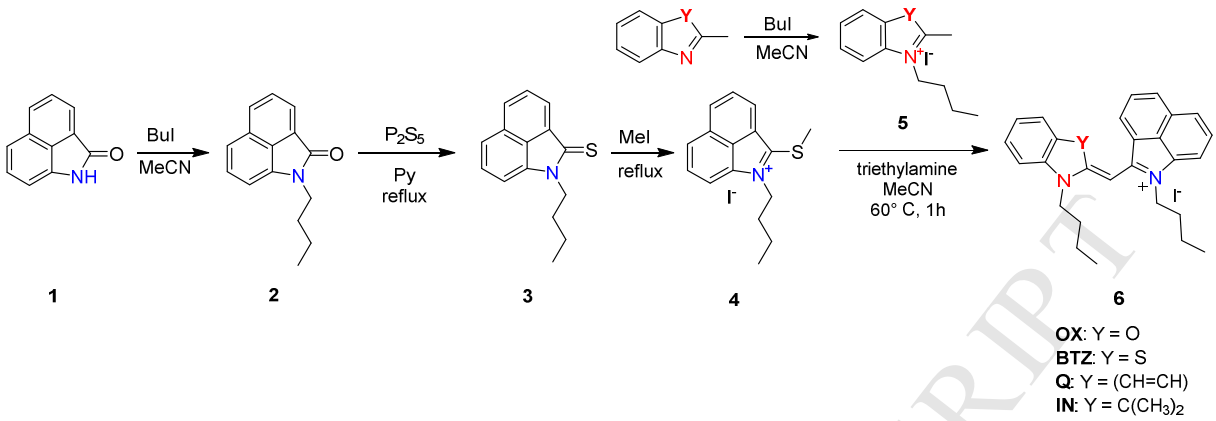

Scheme 1. Synthesis of monomethine cyanines

The condensation of the heterocycles to form monomethine cyanines begins with the deprotonation of the methyl group at the 2 position of the heterocycle. This activated methylene group of the various heterocyclic salts **5** attacks the 2 position of the other thioether heterocycle **4** and displaces the methyl sulfide moiety. Diethyl ether is added to the reaction mixture and red crystals precipitate. The monomethine dyes **6** are then purified by dissolution in a minimal amount of methanol and precipitation in diethyl ether to get an analytically pure sample. Cyanines **6** were characterized by HRMS, ^{1}H and ^{13}C NMR and their optical properties were investigated.

2.2 Optical Properties

Table 2. Energy values and optical properties of the monomethine cyanines

Dye	E. $_{HOMO}$ (eV)	E. $_{LUMO}$ (eV)	λ_{max} (exp.)	λ_{max} (calc.)	ε ($M^{-1}cm^{-1}$)
OX	-8.31	-6.06	500	490	39,900
BTZ	-8.20	-5.60	560	505	30,700
Q	-7.99	-5.96	585	522	35,900
IN	-8.08	-5.87	559	530	25,200

The optical properties of the monomethine cyanines were measured in ethanol. As shown in Table 2 the absorption maxima range from 500 nm in the benzoxazole containing dye **OX** to

585 nm with the increased conjugation of the quinoline system in **Q**. Their molar absorptivities range from 25,000 $M^{-1}cm^{-1}$ in the dimethylindolenine compound **IN** to almost 40,000 $M^{-1}cm^{-1}$ in the benzoxazole compound **OX**. Benzoxazole compounds are known to be brighter. In general, the molar absorptivities are low for monomethine cyanines due to the benz[*c,d*]indole heterocycle present on the other end of the dye, but it is this heterocycle that causes the absorbance to be redshifted about 100 nm from where the dyes would generally absorb if they were symmetrical.[19] Scientists have attempted to approximate wave functions and energies for atoms and ions since the late 1920s.[26] Over the past 90 years there has been significant improvements for predicting behaviors of these systems and more complex ones. The ability to use theoretical calculations to predict optical properties of fluorophores, such as monomethine dyes is a useful tool for screening compounds which can eliminate the need to synthesize them first thus reducing harmful environmental impact. The ability to use theoretical calculations of optical properties for fluorophores, such as monomethine dyes could be useful for the development of viscosity detection fluorophores or bioimaging agents with desirable optical profiles.[18] Previously, we have shown using computational methods that when the dyes are twisted out of plane, the HOMO orbitals are localized around the more conjugated benz[*c,d*]indole heterocycle, preventing conjugation of the system.[18] The dyes were therefore modeled with a restricted dihedral angle to disallow rotation around the methine carbon. Their geometries were optimized using Hartree-Fock dynamic functional theory (HF-DFT) hybrid exchange-correlation functional and B3LYP/6-31G* basis set to predict the energy of the compounds at ground state.[27] The results from our previous paper were confirmed.[18] The predicted HOMO/LUMO energy gaps correspond to the experimentally observed absorption maxima. The lowest energy gap was in dye **Q** at 2.16 eV which is corroborated by also having

most bathochromic absorbance. Dye **OX** had the highest energy gap at 2.50 eV and displayed the most hypsochromic absorbance. Again, the experimental results mostly agree with the trend of the computationally predicted energy gaps showing that these computational methods can be useful as a predictive tool for determining optical properties of the dyes. An example of the predicted energy gaps is shown with dye **OX** in Figure 1. None of these compounds display significant fluorescence unaccompanied in ethanol.

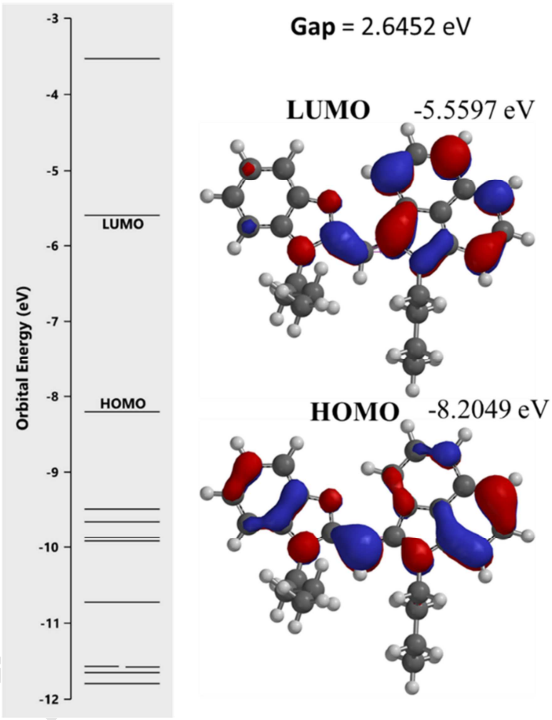

Figure 1. HOMO/LUMO diagrams of **OX**

2.3 DNA Binding

It was previously shown by our lab that only when the monomethine cyanine's ability to rotate around the methine bridge is restricted do the dyes relax by fluorescence.[21] The dyes generally do not fluoresce in free flowing solvent, but when the rotation around the methine bridge is restricted such as in glycerol or when bound, fluorescence can be measured. The

binding of these dyes to ct-DNA restricts this rotation and allows for the unique "turn-on" fluorescence of these compounds.[18] This property was exploited to determine how strongly each heterocycle interacts with DNA compared to the others. Table 3 shows the binding constants and emission maxima of the monomethine cyanines.

Table 3. Binding constants and $\lambda_{emission}$ of monomethine cyanine dyes with various heterocycles

Dye	$\lambda_{emission}$ (nm)	K_b (M^{-1})
OX	555	1.6×10^4
BTZ	583	1.1×10^4
Q	680	1.8×10^2
IN	686	1.6×10^{-3}
TO$^{\alpha}$	525	1.7×10^5

$^{\alpha}$Published values $\lambda_{emission}$[28] and K_b[29]

As shown in Figure 2, dye **OX** displayed the greatest increase in fluorescence when in the presence of ct-DNA with a 700-fold increase. The dye goes from non-fluorescent with no DNA present to almost 700 fluorescence units with 20 μM DNA. This is due to both the binding affinity of the dye (1.6×10^4 M^{-1}) and the tendency of benzoxazole to decrease non-radiative deactivation due to fast intersystem crossing.[30] The benzothiazole containing dye **BTZ** shows a similar binding affinity (1.1×10^4 M^{-1}), but less fluorescence with only about a 40-fold increase. The sulfur atom in benzothiazole can cause the opposite effect of the oxygen in benzoxazole due to a lower singlet-triplet energy gap raising the opportunity for non-radiative relaxation.[19] The change in binding affinity is not very significant, but is likely due to the larger size of the sulfur atom compared to oxygen. This dye is similar to the commercially available dye thiazole orange (TO) which has a binding affinity in the order of 10^5 M^{-1}.[29] TO likely has higher affinity due to steric hinderance of the butyl groups in our dyes as well as the larger size of the

benz[*c*,*d*]indolium heterocycle compared to the quinoline in TO. These values are also on par with similar monomethine cyanine dyes.[31]

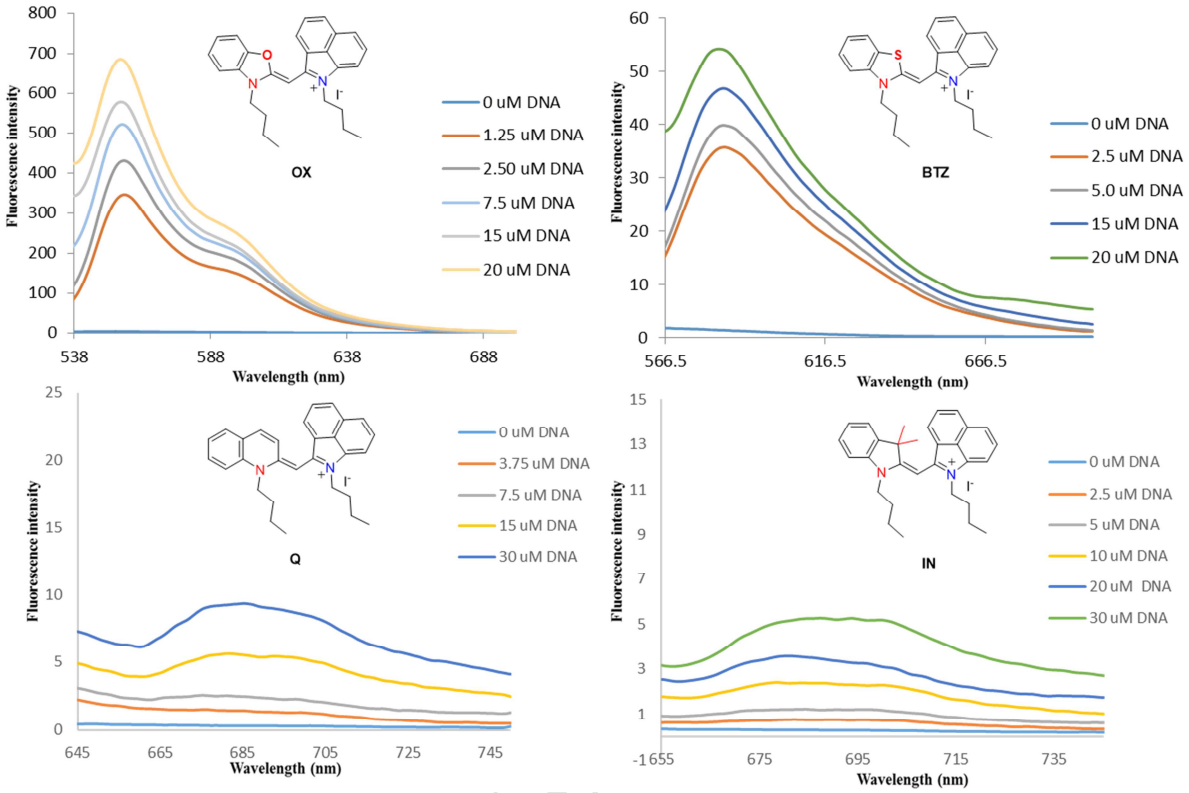

Figure 2. Fluorescence spectrum of monomethine cyanines at constant dye concentration of 10 μM with increasing ct-DNA concentrations from 0-30 μM. The fluorometer reached saturation at 30 μM ct-DNA with dye **OX**.

Unlike the **BTZ** and **OX** compounds which showed excellent binding, the **IN** compound containing a 3,3-dimethylindolenine heterocycle showed almost no binding with a binding affinity of 1.6 x 10^{-3} M^{-1}. This compound was 14 orders of magnitude lower than the benzothiazole and benzoxazole compounds and any binding it may have shown is likely from the benz[*c*,*d*]indole heterocycle on the other side of the dye. As shown in the 3D electrostatic potential maps in Figure 3, dyes **OX** and **BTZ** on the left are planar. As we move to the right, the size of the quinoline in **Q** starts to cause it to rotate slightly out of plane. While the heterocycles

themselves in dye **IN** are flat, the dimethyl groups on the 3,3-dimethylindolenine are perpendicular to the plane of the rest of the dye. Because all the physicochemical properties of the dye have been kept similar and the only change is the dimethyl group, it can be concluded that the perpendicular nature of the dimethyl groups provides steric hindrance that prevents this binding. Our group has reported similar properties with the 3,3-dimethylindolenine preventing duplex DNA binding but still allowing for binding to G-quadruplex DNA in other cyanine classes.[32]

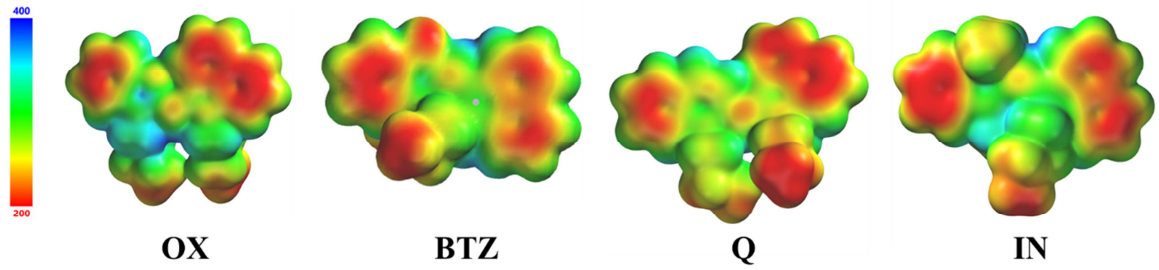

Figure 3. Electrostatic potential maps of monomethine cyanines

This finding is of utmost importance as the dimethyl functionality can be exploited to prevent off site binding in the medicinal applications of these dyes. **OX** could be beneficial as a molecular probe due to its redshifted nature over current commercially available DNA probes (30 nm higher than TO). In addition, this dye should have higher fluorescence intensity than the commercially available probes due to the exclusion of quinoline from the structure. Quinolines are known to experience non-radiative return of decay. These compounds will continue to become more useful as the fluorescence approaches the optical window (650-900 nm) and gets further from the absorption of human tissues.

3. Experimental

3.1 General Information

All chemicals and solvents were of American Chemical Society grade or HPLC purity and were used as received. HPLC grade methanol and glycerol were purchased from Sigma-Aldrich (Saint Louis, MO). All other chemicals were purchased from Fisher Scientific (Pittsburgh, PA, USA) or Acros Organics. The reactions were followed using silica gel 60 F_{254} thin layer chromatography plates (Merck EMD Millipore, Darmstadt, Germany). The ^{1}H NMR and ^{13}C NMR spectra were obtained using high quality Kontes NMR tubes (Kimble Chase, Vineland, NJ) rated to 500 MHz and were recorded on a Bruker Avance (400 MHz) spectrometer DMSO-d_6. High-resolution accurate mass spectra (HRMS) were obtained at the Georgia State University Mass Spectrometry Facility using a Waters Q-TOF micro (ESI-Q-TOF) mass spectrometer. UV-Vis/NIR absorption spectra were recorded on a Varian Cary 50 spectrophotometer interfaced with Cary WinUV Scan Application v3.00 using VWR disposable polystyrene cuvettes with a 1 cm pathlength. Laser Induced Fluorescence (LIF) emission spectra were acquired using Shimadzu RF-5301 Spectroflurophotometer (Shimadzu Corporation Analytical Instruments Division, Duisburg, F. R. Germany) interfaced to a PC with RF-5301PC software using Sigma-Aldrich disposable polystyrene fluorimeter cuvettes with a 1 cm pathlength. All spectral measurements were recorded at room temperature. The data analysis and calculations were carried out using Microsoft Excel (Microsoft Corporation, Redmond, Wa).

3.2 Synthesis

The synthesis of monomethine cyanines was accomplished as reported previously by our group.[18,21]

Compound **4** was previously synthesized by our group and others.[18,21,33]

Each individual heterocycle was dissolved in acetonitrile and refluxed overnight with butyl iodide to form quaternary ammonium salts **5**.

Thioether **4** and each quaternary ammonium salt **5**, respectively, were dissolved in acetonitrile and triethlyamine was added to the solution. The reaction mixture was refluxed at 60 °C for 1 h and monitored by UV-Vis. Upon cooling to room temperature, the corresponding dyes **6** were precipitated by adding diethyl ether. The solid was collected by vacuum filtration and triethylammonium salts were removed by washing with deionized water. The final dyes were purified via precipitation from methanol with diethyl ether.

1-butyl-2-((3-butylbenzo[d]oxazol-2(3H)-ylidene)methyl) benzo[c,d]indol-1-ium iodide, **OX**: Yield 60%; ^{1}H NMR (400 MHz, DMSO-d_6): δ ppm 0.96 (m, 6 H), 1.50 (m, 4 H), 1.83 (m, 4 H) 4.50 (t, *J* = 6.8 Hz, 2 H), 4.61 (t, *J* = 7.2 Hz, 2 H), 6.14 (s, 1 H), 7.62 (m, 4 H), 7.73 (t, *J* = 8.0 Hz, 1 H), 7.88 (d, *J* = 8.0 Hz, 1 H), 7.92 (d, *J* = 7.2 Hz, 1 H), 8.05 (t, *J* = 7.6 Hz, 1 H), 8.17 (d, *J* = 8.0 Hz, 1 H), 9.22 (d, *J* = 7.2 Hz, 1 H); ^{13}C NMR (100 MHz, DMSO-d_6) δ ppm 14.1, 14.2, 19.8, 20.0, 30.3, 30.3, 43.6, 44.9, 75.4, 110.3, 112.4, 112.6, 122.9, 124.6, 126.5, 127.2, 128.4, 129.6, 130.4, 131.1, 132.9, 140.9, 146.9, 155.5, 161.3. HRMS m/z: calc. for $C_{27}H_{29}N_2O^+$ 397.2274, obsd 397.2255.

1-butyl-2-((3-butylbenzo[d]thiazol-2(3H)-ylidene)methyl) benzo[c,d]indol-1-ium iodide, **BTZ**: Yield 65%; ^{1}H NMR (400 MHz, DMSO-d_6): δ ppm 0.966 (m, 6 H), 1.53 (m, 4 H), 1.85 (m, 4 H) 4.40 (t, *J* = 7.2 Hz, 2 H), 4.76 (t, *J* = 7.6 Hz, 2 H), 6.46 (s, 1 H), 7.60 (m, 5 H), 7.90 (t, *J* = 7.6 Hz, 1 H), 8.08 (d, *J* = 8.4 Hz, 1 H), 8.35 (d, *J* = 8.0 Hz, 1 H), 9.34 (d, *J* = 7.2 Hz, 1 H); ^{13}C NMR (100 MHz, DMSO-d_6) δ ppm 14.1, 14.2, 19.9, 20.1, 30.0, 30.2, 43.8, 47.7, 87.2, 109.6, 115.2, 122.5, 124.1, 124.8, 125.7, 127.0, 127.7, 128.2, 129.3, 129.7, 130.0, 132.8, 140.7, 141.3, 154.6, 164.9. HRMS m/z: calc. for $C_{27}H_{29}N_2S^+$ 413.2046, obsd 413.2039.

1-butyl-2-((1-butylbenzo[cd]indol-2(1H)-ylidene)methyl) quinolin-1-ium iodide, **Q**: Yield 69%; ^{1}H NMR (400 MHz, DMSO-d_6): δ ppm 0.98 (m, 6 H), 1.48 (m, 2 H), 1.59 (q, *J* = 7.2 Hz, 2 H), 1.80 (m, 2 H), 1.94 (m, 2 H), 4.25 (t, *J* = 7.2 Hz, 2 H), 4.88 (t, *J* = 7.2 Hz, 2 H), 6.23 (s, 1 H), 7.33 (m, 1 H), 7.62 (m, 3 H), 7.83 (t, *J* = 7.6 Hz, 1 H), 8.10 (m, 2H), 8.23 (d, *J* = 8.0 Hz, 1 H), 8.32 (d, *J* = 7.2 Hz, 1 H), 8.39 (d, *J* = 8.0 Hz, 1 H), 8.67 (m, 2 H); ^{13}C NMR (100 MHz, DMSO-d_6) δ ppm 14.0, 14.2, 19.8, 20.2, 30.0, 30.1, 43.3, 51.1, 92.5, 106.8, 118.7, 120.5, 124.3, 125.0, 125.8, 127.7, 128.0, 129.4, 129.9, 130.3, 130.4, 130.3, 130.4, 130.9, 134.6, 139.2, 142.0, 142.5, 152.9, 156.4. HRMS m/z: calc. for $C_{29}H_{31}N_2^+$ 407.2482, obsd 407.2463.

1-butyl-2-((1-butyl-3,3-dimethylindolin-2-ylidene)methyl)benzo[cd]indol-1-ium iodide, **IN**: Yield 72%; mp 220-222 °C; ^{1}H NMR (400 MHz, DMSO-d_6): δ ppm 0.63 (t, *J* = 7.6 Hz, 3 H), 0.92 (t, *J* = 7.2 Hz, 3 H), 1.01 (m, 2 H), 1.40 (m, 2 H), 1.46 (m, 2 H), 1.60 (s, 6 H), 1.82 (m, 2 H), 4.19 (t, *J* = 6.4 Hz, 2 H), 4.50 (t, *J* = 7.2 Hz, 2 H), 7.43 (t, *J* = 7.2 Hz, 1 H), 7.57 (t, *J* = 7.2 Hz, 1 H), 7.74 (m, 4 H), 7.89 (m, 2 H), 8.01 (d, *J* = 7.6 Hz, 1 H) 8.36 (d, *J* = 8.0 Hz, 1 H); ^{13}C NMR (100 MHz, DMSO-d_6) δ ppm 13.7, 14.1, 19.1, 19.9, 26.2, 29.7, 30.3, 44.1, 50.6, 52.1, 84.3, 111.5, 114.8, 123.6, 123.7, 124.3, 126.8, 128.9, 128.9, 129.7, 130.0, 130.5, 130.5, 133.2, 141.0, 141.1, 142.2, 156.3, 180.9. HRMS m/z: calc. for $C_{30}H_{35}N_2^+$ 423.2795, obsd 397.2773.

3.3 Computational Methods

The structure of each compound was first optimized using the HF-DFT method with the hybrid exchange-correlation functional, B3LYP/6-31G* basis set using Spartan '14 (Irvine, CA).[34] The torsional angles from the quaternary nitrogen to the α-carbon on the alternate heterocycle were restricted to 180° to get the calculated absorbance values, HOMO and LUMO orbitals, physicochemical properties and electrostatic potential maps. The electrostatic potential

maps and the calculated HOMO and LUMO orbitals were obtained using a restricted hybrid HF-DFT, self-consistent field in vacuum performed with B3LYP/6-31G* basis set.

3.3 Stock Solutions

Stock solutions were prepared by weighing the solid of each individual compound on a 5-digit analytical balance and adding solvent via class A volumetric pipette to make a 1.0 mM solution. The vials were vortexed for 20 s and then sonicated for 5 min to ensure complete dissolution. When not in use, the stock solutions were stored in the dark at 4 °C.

3.4 Method of Determining Absorbance and Fluorescence

Stock solutions were used to prepare five dilutions of dyes with concentrations ranging from 5-25 μM using a class A volumetric pipette in order to maintain absorption between 0.1 and 1.0. The dye solutions were diluted ten-fold for fluorescence in order to minimize inner filter effect. The absorption spectra of each sample were measured in duplicate from 400 to 750 nm. The emission spectra of each sample were measured in duplicate with a 530 nm excitation wavelength and slit widths of 5 nm for both excitation and emission. Emission spectra were corrected by the developed method file.

3.5 DNA Binding Studies

A stock solution of each dye ($1x10^{-4}$ M) and ct-DNA type 1 ($7.5x10^{-3}$ M) were prepared in ethanol and Tris-HCl buffer solution, respectively. Fluorescence titration with ct-DNA concentrations (0-200 mM) were made by mixing 35 μL dye solution with Tris-HCl buffer solution with and without ct-DNA to a total volume of 3500 μL in a fluorescence cuvette to make working solutions of 10 μM. Fluorescence spectra were measured in duplicate with excitation at 530 nm and slit widths of 5 nm for both excitation and emission.

4. Conclusion

A series of monomethine cyanines were synthesized in good yield with red-shifted absorbance properties in comparison to previously synthesized monomethine cyanine dyes. Although the benz[*c,d*]indolium containing monomethine cyanine dyes in this report are non-fluorescent in free flowing solvent, their fluorescence is "turned on" through the restriction of the methine bridge caused by binding to DNA. Computational methods were shown to be useful as a predictive tool for determining their optical properties. In keeping everything the same except for a single heterocycle, binding affinity to ct-DNA of these heterocycles were able to be compared. **OX** stood out as the best candidate as a starting point for building a new molecular probe due to its strong binding affinity and 700-fold increase in fluorescence from binding. In addition, **IN** with a 3,3-dimethylindolenine heterocycle showed almost no binding due to the steric hindrance of the dimethyl group. This could be exploited to prevent offsite binding. Utilizing the described techniques these dyes could be further developed as potential biological probes. Future studies will investigate how different substitutions on the heterocycles could increase binding affinities and increase optical activity to various biological targets.

Acknowledgements

MH, AL, CH and ES would like to thank the Department of Chemistry at Georgia State University for their support and the funds provided for the Ph.D. dissertation of AL. MH wishes to thank the Brains and Behavior Seed Grant, the Health Innovation Program Grant and Atlanta Clinical & Translational Science Institute and the Georgia Research Alliance Grant for their support.

References

(1) Williams, C. G. —Researches on Chinoline and its Homologues. Earth Environ. Sci. Trans. R. Soc. Edinb. 1857, 21, 377–401.

(2) Choi, H. S.; Nasr, K.; Alyabyev, S.; Feith, D.; Lee, J. H.; Kim, S. H.; Ashitate, Y.; Hyun, H.; Patonay, G.; Strekowski, L.; Henary, M.; Frangioni, J. V. *Angew Chem Int Edit* **2011**, *50*, 6258.

(3) Ashitate, Y.; Levitz, A.; Park, M. H.; Hyun, H.; Venugopal, V.; Park, G.; El Fakhri, G.; Henary, M.; Gioux, S.; Frangioni, J. V.; Choi, H. S. *Chem Commun (Camb)* **2016**, *52*, 10305.

(4) Hyun, H.; Owens, E. A.; Wada, H.; Levitz, A.; Park, G.; Park, M. H.; Frangioni, J. V.; Henary, M.; Choi, H. S. *Angew Chem Int Ed Engl* **2015**, *54*, 8648.

(5) Hany, R.; Fan, B.; de Castro, F. A.; Heier, J.; Kylberg, W.; Nuesch, F. *Prog Photovoltaics* **2011**, *19*, 851.

(6) Malinkiewicz, O.; Grancha, T.; Molina-Ontoria, A.; Soriano, A.; Brine, H.; Bolink, H. J. *Adv Energy Mater* **2013**, *3*, 472.

(7) Li, J.; Gan, F. X. *Appl Optics* **2000**, *39*, 3525.

(8) Shi, Q. Q.; Sun, R.; Ge, J. F.; Xu, Q. F.; Li, N. J.; Lu, J. M. *Dyes Pigments* **2012**, *93*, 1506.

(9) Ajayaghosh, A. *Accounts Chem Res* **2005**, *38*, 449.

(10) Warner, I. M.; Soper, S. A.; McGown, L. B. *Anal Chem* **1996**, *68*, R73.

(11) Haugland, R. P.; Spence, M. T. Z.; Johnson, I. D. *Handbook of fluorescent probes and research chemicals*; 6th ed.; Molecular Probes: Eugene, OR, USA (4849 Pitchford Ave., Eugene 97402), 1996.

(12) Deligeorgiev, T. G.; Zaneva, D. A.; Kim, S. H.; Sabnis, R. W. *Dyes Pigments* **1998**, *37*, 205.

(13) El-Shishtawy, R. M.; Asiri, A. M.; Basaif, S. A.; Rashad Sobahi, T. *Spectrochim Acta A Mol Biomol Spectrosc* **2010**, *75*, 1605.

(14) Lakowicz, J. R. *Principles of fluorescence spectroscopy*; 3rd ed.; Springer: New York, 2006.

(15) Kantor, G. J.; Hull, D. R. *Biophys J* **1979**, *27*, 359.

(16) Cerutti, P. A. *Science* **1985**, *227*, 375.

(17) Marks, R. *Cancer* **1995**, *75*, 607

(18) Soriano, E.; Holder, C.; Levitz, A.; Henary, M. *Molecules* **2015**, *21*, E23.

(19) Levitz, A.; Ladani, S. T.; Hamelberg, D.; Henary, M. *Dyes and Pigments* **2014**, *105*, 238.

(20) Gibas, C.; Kretschy, N.; Somoza, M. M. *Plos One* **2014**, *9*, e85605.

(21) Soriano, E.; Outler, L.; Owens, E. A.; Henary, M. *Journal of Heterocyclic Chemistry* **2015**, *52*, 180.

(22) Flors, C. *Biopolymers* **2011**, *95*, 290.

(23) Timcheva, II; Maximova, V. A.; Deligeorgiev, T. G.; Gadjev, N. I.; Sabnis, R. W.; Ivanov, I. G. *FEBS Lett* **1997**, *405*, 141.

(24) Timtcheva, I.; Maximova, V.; Deligeorgiev, T.; Zaneva, D.; Ivanov, I. *Journal of Photochemistry and Photobiology A: Chemistry* **2000**, *130*, 7.

(25) Karlsson, H. J.; Eriksson, M.; Perzon, E.; Akerman, B.; Lincoln, P.; Westman, G. *Nucleic Acids Res* **2003**, *31*, 6227.

(26) Schrödinger, E. *Physical Review* **1926**, *28*, 1049.

(27) Stephens, P. J.; Devlin, F. J.; Chabalowski, C. F.; Frisch, M. J. *The Journal of Physical Chemistry* **1994**, *98*, 11623.

(28) Nygren, J.; Svanvik, N.; Kubista, M. *Biopolymers* **1998**, *46*, 39.

(29) Ghasemi, J.; Ahmadi, S.; Ahmad, A. I.; Ghobadi, S. *Appl Biochem Biotechnol* **2008**, *149*, 9.

(30) Reiser, A.; Leyshon, L. J.; Saunders, D.; Mijovic, M. V.; Bright, A.; Bogie, J. *Journal of the American Chemical Society* **1972**, *94*, 2414.

(31) El-Shishtawy, R. M.; Asiri, A. M.; Basaif, S. A.; Rashad Sobahi, T. *Spectrochimica Acta Part A: Molecular and Biomolecular Spectroscopy* **2010**, *75*, 1605.

(32) Nanjunda, R.; Owens, E.; Mickelson, L.; Dost, T.; Stroeva, E.; Huynh, H.; Germann, M.; Henary, M.; Wilson, W. *Molecules* **2013**, *18*, 13588.

(33) Sinha, S. H.; Owens, E. A.; Feng, Y.; Yang, Y.; Xie, Y.; Tu, Y.; Henary, M.; Zheng, Y. G. *Eur J Med Chem* **2012**, *54*, 647.

(34) Shao, Y.; Molnar, L. F.; Jung, Y.; Kussmann, J.; Ochsenfeld, C.; Brown, S. T.; Gilbert, A. T. B.; Slipchenko, L. V.; Levchenko, S. V.; O'Neill, D. P.; DiStasio Jr, R. A.; Lochan, R. C.; Wang, T.; Beran, G. J. O.; Besley, N. A.; Herbert, J. M.; Yeh Lin, C.; Van Voorhis, T.; Hung Chien, S.; Sodt, A.; Steele, R. P.; Rassolov, V. A.; Maslen, P. E.; Korambath, P. P.; Adamson, R. D.; Austin, B.; Baker, J.; Byrd, E. F. C.; Dachsel, H.; Doerksen, R. J.; Dreuw, A.; Dunietz, B. D.; Dutoi, A. D.; Furlani, T. R.; Gwaltney, S. R.; Heyden, A.; Hirata, S.; Hsu, C.-P.; Kedziora, G.; Khalliulin, R. Z.; Klunzinger, P.; Lee, A. M.; Lee, M. S.; Liang, W.; Lotan, I.; Nair, N.; Peters, B.; Proynov, E. I.; Pieniazek, P. A.; Min Rhee, Y.; Ritchie, J.; Rosta, E.; David Sherrill, C.; Simmonett, A. C.; Subotnik, J. E.; Lee Woodcock Iii, H.; Zhang, W.; Bell, A. T.; Chakraborty, A. K.; Chipman, D. M.; Keil, F. J.; Warshel, A.; Hehre, W. J.; Schaefer Iii, H. F.; Kong, J.; Krylov, A. I.; Gill, P. M. W.; Head-Gordon, M. *Phys. Chem. Chem. Phys.* **2006**, *8*, 3172.

A series of monomethine cyanines were synthesized in good yield with red-shifted absorbance properties

Computational methods were shown to be useful as a predictive tool for determining their optical properties

The dyes displayed “turn-on” fluorescence when bound to ct-DNA

One of these dyes, **OX**, displayed a 700-fold increase in fluorescence when bound to 20 μM ct-DNA